

# Multidisciplinary Analysis to Interpret the Palaeoclimate and Depositional Environment of the Late Paleozoic Post-glacial Sediments from Wardha Basin, Maharashtra, Central India

Pauline Sabina Kavali<sup>1\*</sup>, Mercedes di Pasquo<sup>2</sup> and Shobhit Kumar Kushwaha<sup>3</sup>

<sup>1</sup>Birbal Sahni Institute of Palaeosciences, 53 University Road Lucknow, 226 007 Uttar Pradesh State, India.

<sup>2</sup>Laboratorio de Palinoestratigrafía y Paleobotánica, CICYTTP- Pcia. E. R.-UADER (Centro de Investigaciones Científicas y Transferencia de Tecnología a la Producción- Entre Ríos-Universidad Autónoma de Entre Ríos), CONICET (Consejo Nacional de Investigaciones Científicas y Tecnológicas), España 149, E3105BWA Diamante, Entre Ríos, Argentina.

<sup>3</sup>Institute of Hydrocarbon Energy and Geo Resources, Department of Applied Geology, University of Lucknow 226 007, India.

\*E-mail: kpauline\_sabina@bsip.res.in

Received: 23 June 2022 / Revised form Accepted: 9 November 2022

© 2023 Geological Society of India, Bengaluru, India

## ABSTRACT

A multidisciplinary analysis has been applied to subsurface samples from borehole MAWP 114, Wardha basin, Maharashtra State, central India, in order to characterize the palaeoclimatic and local depositional conditions during the deposition of the Permo-Carboniferous Talchir Formation. Based on palynology, palynofacies, TOC (Total organic carbon) and  $\delta^{13}\text{C}$  analyses five types of palaeoclimatic phases and local depositional conditions have been envisaged within the studied sequence. In palynofacies type I (P-I), the dominance of AOM and scarce palynomorphs of upland xerophytic affinity (represented by primitive conifers such as *Potonieisporites*) suggests deposition during the earliest phase of a glacial retreat in distal anoxic conditions. In P-II dominance of AOM with moderate increase in palynomorphs and phytoclasts suggests amelioration in climate and deposition during a mid interglacial phase under dysoxic to suboxic conditions. In P-III, increase in palynomorphs and phytoclasts and decrease in AOM suggests deposition in a median distal to proximal setting under warm temperate conditions during late interglacial phase. P-I to P-III have been demarcated in a shale sequence. P-IV is demarcated in the overlying sandstone-shale intercalation, characterized by predominance of non-opaque phytoclasts of the pitted and banded type, subdominance of spore and pollen and low frequency of AOM and suggests deposition in proximal oxic conditions during final deglacial phase under high energy settings. P-V recognized in sandstones, comprising of dominance of terrestrial AOM and scarce palynomorphs and phytoclasts suggests deposition in post glacial fluvial, under anoxic to dysoxic setting. These climatic shifts are also supported by geochemical results from TOC (0.3%-2.2%) and  $\delta^{13}\text{C}$  (-24.9‰ to -21.4‰) analyses, as both reflect palaeo-atmospheric fluctuations in accordance with direct impact of glaciation and deglaciation episodes on biotic communities along the studied interval.

## INTRODUCTION

The late Carboniferous and early Permian interval is best to analyse response of vegetation to glacial-interglacial oscillations, as

it records the transition from cold to warm-climate conditions well-established in the mid- late Permian (Shi and Waterhouse, 2010). Montañez and Poulsen (2013) have shown that changes in the compositions of terrestrial flora, marine fauna and geographic patterns are indicative of responses to glacial conditions in high-latitude. Throughout the late Carboniferous and early Permian Gondwana witnessed a periglacial to cool-temperate climate as well as monsoonal phases (Parrish, 1990; Scotese et al., 2021). The Gondwanan sedimentary basins document evidences of several interglacial phases, which lead to the establishment of marine, lacustrine, deltaic and fluvial environments, during which plant associations succeeded themselves reflecting ecologic- evolutionary aspect (Bernardes-de-Oliveira et al., 2016).

In India, the late Palaeozoic glaciation is recorded in the Permo-Carboniferous Talchir Formation, which is the oldest stratigraphic unit of the Gondwana Supergroup. Blanford et al., (1856) designated Talchir Group to its deposits in the Talchir basin in the State of Odisha. Climate sensitive lithologies of this unit allowed the recognition of different paleoenvironments associated to glacial and deglacial processes such as glacio-fluvial and glacio-lacustrine (Banerjee, 1966; Ghosh and Mitra, 1975), and glacio-marine (Bose et al., 1992; Mukhopadhyay and Bhattacharya 1994; Bhattacharya et al., 2002, 2004, 2005, 2009; Bhattacharya, 2003, 2013; Chakraborty and Bhattacharya, 2005; Bhattacharya and Bhattacharya, 2006, 2007, 2010, 2011, 2012, 2014, 2015). Under the impact of climatic changes, the floristic Gondwana province underwent a transformation with regard to its composition and geographic distribution and several authors have proposed different climatic divisions in India. Vijaya (1994) recognised three phases in the Talchir Formation due to increase in microfloral diversity up section: Phase I- Asselian, with common monosaccate pollen both radially- and bilaterally-symmetrical and non-sculptured trilete spores. Phase II- by monosaccate sculptured pollen, bisaccate taeniate pollen and sculptured spores. Phase III- early Sakmarian, manifesting higher diversity of forms. Such phases reflecting climatic amelioration were also shown by Banerjee and D'Rozario (1990), Tiwari (1994), Venkatachala et al., (1995), Pant (1996) and Vijaya et al., (2001). With some limitations, and considering

the chronologic changes around the latest Pennsylvanian and the Asselian of the early Permian that occurred in the last three decades (see Ogg et al., 2016), these phases can be identified in glacial-deglacial sequences elsewhere in Gondwana (e.g. MacRae 1988; Stephenson et al., 2005, 2007, 2013; Stephenson, 2008; Modie and Le Herissé, 2009; Iannuzzi, 2013; Limarino et al., 2014; di Pasquo et al., 2017; Beri et al., 2019; Valdez et al., 2020; Backhouse and Mory, 2020; Souza et al., 2021 and references therein).

Here the nature of climate–vegetation interaction during transition from late Pennsylvanian-early Permian in Talchir Formation is assessed which is located in the southern temperate high palaeolatitude Indian Gondwana sequences and the depositional setting of the succession studied. The present contribution focuses on the analysis of palynofacies and botanical affinities of spore-pollen content and geochemical trends of stable organic carbon isotope and TOC obtained from subsurface sediments of borehole MAWP 114, in the Wardha basin, Maharashtra state, Central India (Fig. 1A and B). These analyses let us interpret the linkage between vegetation and climate shifts in response to glacial-interglacial fluctuations in this temperate region of Gondwana, as well as their local depositional conditions.

## GEOLOGICAL SETTING

Following a long depositional hiatus since the Proterozoic, India entered the South Pole circle (Roy and Purohit, 2018) during the Permo-Carboniferous period and sedimentation resumed by the Pangea relaxation (Veevers and Tewari, 1995), and the Gondwanan rift basins were opened, which led to depressions (broad depocenters) filled with rock debris from melting glaciers and other deposits related to glaciation and deglaciation processes.

Therefore, these Indian Gondwana basins preserve a 200 Ma thick sedimentary succession from the latest Carboniferous to the Early Cretaceous (Mukhopadhyay et al., 2010). The nature of the Gondwana sediments was broadly controlled by three common factors: granitic provenance, the basal unit of glacial origin, and the fluvial nature of the rest of the overlying succession that largely deposited fluvio-deltaic, fluvio-lacustrine, and alluvial sediments (Acharyya, 2019a). The upper Carboniferous to Permian stratigraphic succession is represented by the glaciogene Talchir Formation, and the overlying carbonaceous shale and coal-bearing deposits of Damuda, followed by Mesozoic

greenhouse interval represented by the Panchet and its equivalent formations, composed of feldspathic sandstone and red claystone, and the Mahadeva or the Supra-Panchet ones bearing rare feldspar, quartz-arenite and variegated claystones (Acharyya, 2019a).

The Gondwana sedimentary basins are distributed along four major belts such as E-W Satpura-Son-Damodar, NNW-SSE Wardha-Godavari, NNW-SSE Mahanadi and N-S Rajmahal- Birbhum (Fig. 1A). The nature of the upper Paleozoic succession was determined by a combination of climate change, local environmental conditions and tectonic activities, especially related to inherited fabrics of deformation from reactivation of the shear zones and faults settled in the Precambrian basement (Acharyya, 2019a). These geodynamic processes terminated with the Gondwanan break up in the Mesozoic indicated by flooding basalts and mafic and ultramafic intrusions (Acharyya, 2019b).

The Wardha Basin lies in the north eastern part of Maharashtra state bordering the states of Madhya Pradesh and Telangana, between N19°14'39.48", E79°8'27.88" with an estimated area of 4000 km<sup>2</sup>. It extends southeastward into Godavari basin in Telangana State (Fig. 1a). Toward the east, the Gondwana deposits are bordered by the Archaean rocks. Towards the northeast, southwest, and southeast the Precambrian Vindhyan Formation occurs in between the outlines of the faults of coal-bearing deposits. The Talchir Formation lies in the central part around the core of which lies the coal of the Barakar Formation in an elliptical pattern. The Barakar Formation occurs in isolated patches in the western part and is overlain by the Kamthi Formation. Towards the west and north the Deccan trap covers the Gondwana sediments. Towards the north are also patches of Lameta Formation. The borehole MAWP 114 herein studied was drilled in Penganga area of Wardha valley coalfield, Chandrapur district (Fig 1B).

## MATERIALS AND METHODS

The borehole MAWP 114 intersected in descending order, the upper Permian Kamthi (3-78 m), the middle Permian Motur (78-294 m), the lower Permian Barakar (294-469.50 m) and the Permo-Carboniferous Talchir (469.51-471 m) formations, and unconformably, the Precambrian basement represented by limestones of the Vindhyan Group. The interval studied for palynology and geochemical analysis

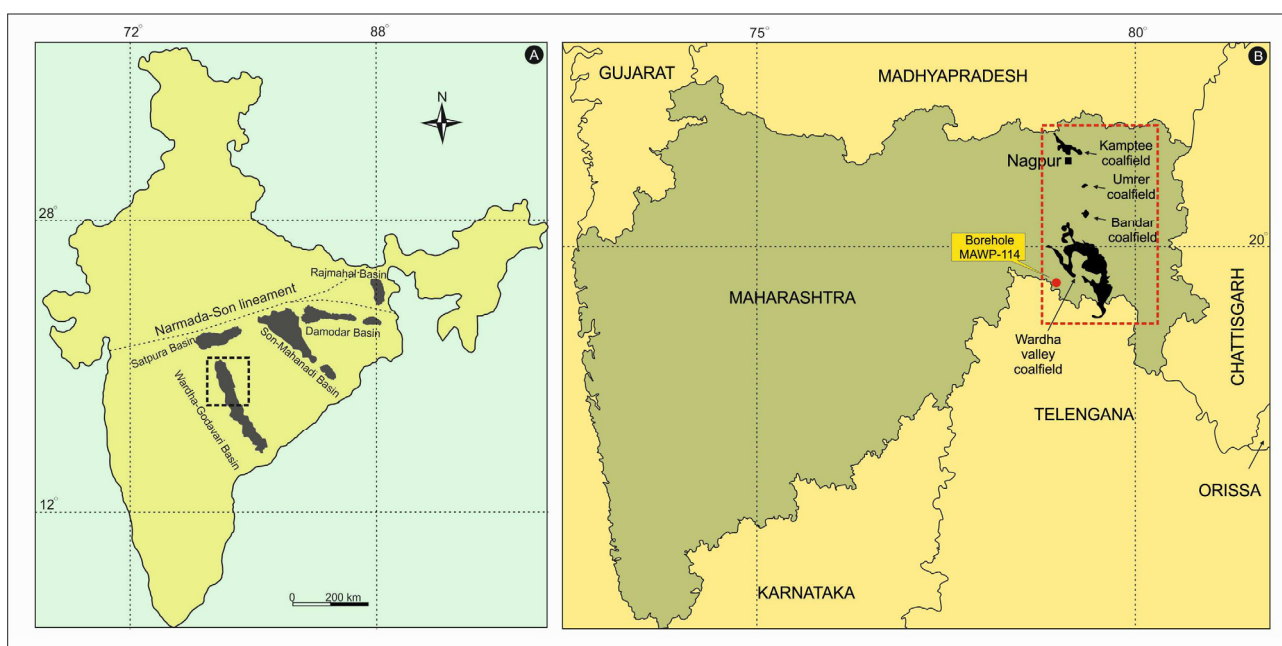


**Fig. 1.** A. Map showing the Gondwana basins in India (after Geological Survey of India). B. Map of Maharashtra State showing the coalfields in the Wardha Basin and the location of MAWP 114 Borehole of the present study.

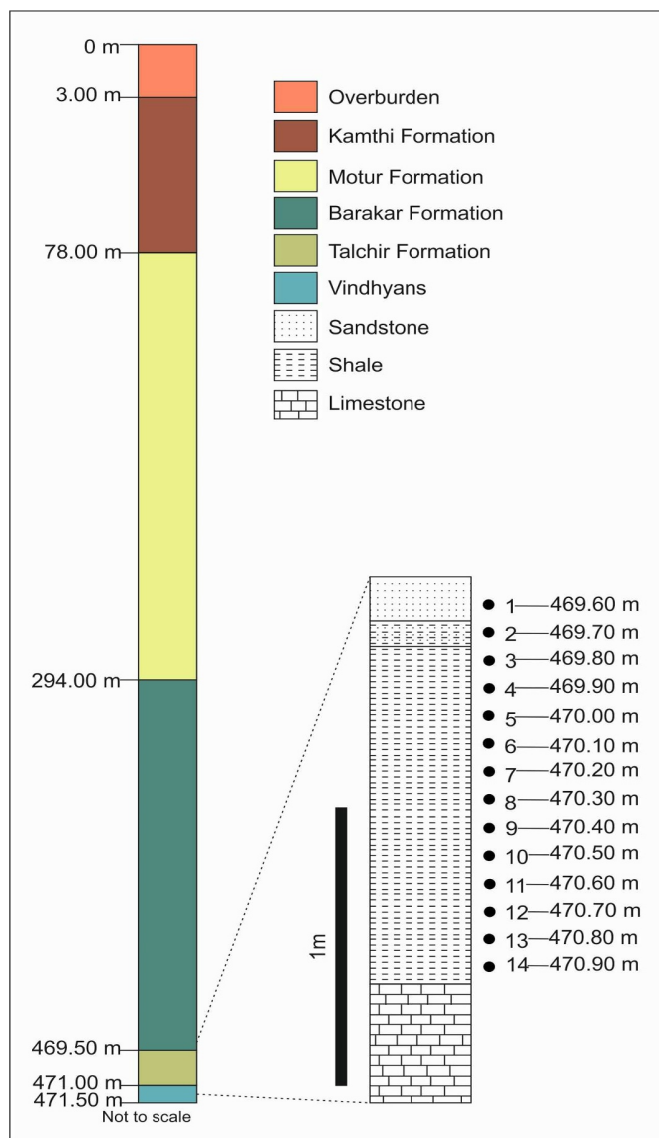


**Fig. 2.** Litholog of MAWP 114 Borehole showing the position of samples studied.

is represented by 14 samples of the Permo-Carboniferous Talchir Formation (Fig. 2).

For palynological analyses and organic matter characterization the borehole samples were treated according to standard procedures including 10% hydrochloric acid (HCl), 40% hydrofluoric acid (HF). The organic residues were sieved over a 500 micron sieve and slides mounted with Canada balsam. The samples were processed at the Birbal Sahni Institute of Palaeosciences, Lucknow where the materials are stored in the museum repository under the codes BSIP 16718-16739. The microscopic examination of slides carried out under an Olympus BX61 microscope bearing a DP-25 digital camera with Cell A software.

Despite rather subjective, palynomorphs were classified following several workers and their botanical affinities indicated (Balme, 1970, 1995; Archangelsky and Gamero, 1979; Foster 1979; Backhouse, 1991; Azcuy and di Pasquo, 2000; Playford and Dino 2000a, 2000b; di Pasquo and Grader, 2012; di Pasquo et al., 2021; Kavali et al., 2021 and references therein). The classification of organic components and palynomorphs allowed the counting of a minimum of 300 particles per sample. A semi-quantitative approach was carried out under 20x magnification and a visual estimation of the relative abundances of palynological organic components expressed as percentages of PM.

The classification of kerogen applied by Tyson (1995) and Mendonça-Filho et al., (2010) was used, which include three main

groups of morphologic constituents: phytoclasts, palynomorphs and amorphous organic matter. In agreement with these authors, the phytoclast group includes fragments of tissues derived from higher plants, fungi or other remains, translucent (non-opaque) or opaque (black) and non-biostructured or biostructured (tracheids, cuticles, membranes of striate, striped, pitted or banded type) or even “pseudoamorphous”. The amorphous matter is composed of diagenetically derived algae or intense biodegradation of any organic product of both terrestrial and/or marine sources. The graphs were prepared using Microsoft Excel and Corel draw XVII.

The sample preparation for carbon isotopic analysis followed procedures applied by Agrawal et al., (2015, 2017). TOC was calculated from the peak obtained from the sum of the integrated  $m/z$  44, 45 and 46 signal measured in the CF-IRMS (Jensen, 1991). These analyses were carried out at the stable isotope facility at BSIP, Lucknow, India.

## RESULTS AND INTERPRETATION

All the 14 samples from the Permo-Carboniferous Talchir Formation of bore hole MAWP114 were productive. A total of 29 palynotaxa composed of trilete spores (13) and pollen grains (16) chiefly monosaccate and bisaccate type (Table 1), derived from lycophytes and monilophytes (pteridophytes and sphenophytes) and several gymnosperm groups (Cordaitalean, Coniferalean, Ginkgo/Cycadalean, Pteridosperms) have been recorded (Fig. 3). Based on the palynofacies components and pollen and spore frequencies along with that of the chlorophycean *Botryococcus* (Fig. 4) allowed the characterization of five palynofacies types illustrated in Fig. 5. The results from Carbon isotope ( $\delta^{13}C$ ) and TOC analysis are given in Fig. 6 A and B.

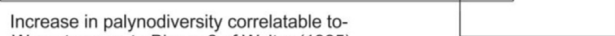
On the basis of the qualitative and quantitative results obtained from palynological, palynofacies and Carbon isotope ( $\delta^{13}C$ ) and TOC analyses, paleoenvironmental stages could be demarcated (Fig. 3) and their local depositional settings inferred.

### Earliest Phase of a Glacier Retreat

The Phase 1 can be related to sub-polar climate with cold-arid conditions, wherein a tundra-type vegetation must have covered the landscape and vegetation would be similar to modern Cold temperate Biome 8 of Walter (1985). Glaciation resulted in sea-level fall and climatic aridity. Low diverse floras represented by sparse xeromorphic allochthonous conifers such as late Pennsylvanian *Potonieisporites*, characterize drier habitats in this phase, probably as a consequence of changing continental configurations during the late Pennsylvanian and the intensity of glaciation at the poles (Phillips and Peppers, 1984; Ziegler, 1990). These primitive conifers are indicative of floras from seasonally-dry habitats (DiMichelle et al., 2010). They reflect a moisture deficit landscape (Knoll, 1985; DiMichelle et al., 2001). Such extrabasinal elements could have been transported to the depocenter in the basin by wind (Farley, 1988; Zhou, 1994; Peppers, 1997; Falcon-Lang, 2004; Dimitrova and Cleal, 2007; DiMichelle et al., 2010) as well as water as they are structurally competent to withstand long distance transport by fluvial agents, and in this case, glacial meltwater. The fragmentary nature of the pollen grains in the assemblages of this phase was due to mechanical disintegration in the course of long distance transportation before final deposition, and not by maceration processes at laboratory. This was confirmed by processing uncrushed larger pieces of shale samples (some larger than 5 cm). However, the residue yielded similar fragmented grains. The depositional setting for these shale samples is interpreted as a distal part of a sandur (outwash) plain, which is formed by sediments carried by meltwater streams that issue from glacial snouts mostly during summers, either in the proglacial region or downstream, several kilometres from the ice margin depending upon the local topography. Krigstrom (1962)

**Table 1.** Distribution of taxa and demarcation of Biomes of Walter (1985) encountered in the present study (For sample details see Figure 2). Sample number and their corresponding BSIP museum repository number. **Sample 1:** 16738-16739; **Sample 2:** 16737; **Sample 3:** 16736; **Sample 4:** 16735; **Sample 5:** 16734; **Sample 6:** 16733; **Sample 7:** 16732; **Sample 8:** 16731; **Sample 9:** 16730; **Sample 10:** 16729; **Sample 11:** 16727-16728; **Sample 12:** 16724-16726; **Sample 13:** 16722-16723; **Sample 14:** 16718-16721.

| Taxa/Sample no                        | 1 | 2 | 3 | 4 | 5 | 6 | 7 | 8 | 9 | 10 | 11 | 12 | 13 | 14 |
|---------------------------------------|---|---|---|---|---|---|---|---|---|----|----|----|----|----|
| <b>Lycophytes</b>                     |   |   |   |   |   |   |   |   |   |    |    |    |    |    |
| <i>Cristatisporites conatus</i>       | P | P | P | P | P | P | P | P | P | P  |    | P  |    |    |
| <i>Cristatisporites pseudozonatus</i> | P | P | P | P |   |   |   |   |   |    |    |    |    |    |
| <i>Indotriradites korbaensis</i>      | P |   |   |   |   |   |   |   |   |    |    |    |    |    |
| <i>Lunbladispora</i> sp.              |   |   |   |   |   |   | P |   |   |    |    |    |    |    |
| <b>Sphenophytes</b>                   |   |   |   |   |   |   |   |   |   |    |    |    |    |    |
| <i>Calamospora hartungiana</i>        |   |   | P | P | P | P | P | P | P | P  |    | P  |    |    |
| <b>Filicophytes</b>                   |   |   |   |   |   |   |   |   |   |    |    |    |    |    |
| <i>Punctatisporites gretensis</i>     | P | P | P | P | P | P | P | P | P | P  | P  | P  |    |    |
| <i>Punctatisporites fungosus</i>      |   |   | P | P | P | P | P | P | P | P  |    | P  |    |    |
| <i>Punctatisporites priscus</i>       |   |   | P | P | P | P | P | P | P | P  |    | P  |    |    |
| <i>Brevitriletes cornutus</i>         |   |   |   |   |   |   |   |   |   |    |    | P  |    |    |
| <i>Horriditriletes ramosus</i>        | P |   | P | P | P | P | P | P | P | P  |    | P  |    |    |
| <i>Leiotriletes directus</i>          |   |   | P | P | P | P | P | P | P | P  |    | P  |    |    |
| <i>Leiotriletes virkki</i>            |   |   | P | P | P | P | P | P | P | P  |    | P  |    |    |
| <i>Verrucosiporites verrucosus</i>    |   |   |   |   |   |   |   |   |   |    |    | P  |    |    |
| <b>GYMNOSPERMS: Pteridosperms</b>     |   |   |   |   |   |   |   |   |   |    |    |    |    |    |
| <i>Protohaploxypinus limpidus</i>     | P | P | P | P | P | P | P | P | P | P  |    | P  |    |    |
| <i>Protohaploxypinus pennatulus</i>   | P | P | P | P | P | P | P | P | P | P  |    | P  |    |    |
| <i>Vittatina subsaccata</i>           |   |   |   |   |   |   |   |   |   |    |    | P  |    |    |
| <b>Ginkgoales</b>                     |   |   |   |   |   |   |   |   |   |    |    |    |    |    |
| <i>Cycadopites cymbatus</i>           | P | P | P | P | P | P | P | P | P | P  |    |    |    |    |
| <b>Cordaitales</b>                    |   |   |   |   |   |   |   |   |   |    |    |    |    |    |
| <i>Canannaropollis janakii</i>        | P | P | P | P | P | P | P | P | P | P  | P  | P  |    |    |
| <i>Canannaropollis densus</i>         | P | P | P | P | P | P | P | P | P | P  |    | P  |    |    |
| <i>Canannaropollis triangularis</i>   | P | P | P | P | P | P | P | P | P | P  |    | P  |    |    |
| <i>Plicatipollenites malabarensis</i> | P | P | P | P | P | P | P | P | P | P  |    | P  |    |    |
| <i>Plicatipollenites gondwanensis</i> | P | P | P | P | P | P | P | P | P | P  |    | P  |    |    |
| <b>Coniferales</b>                    |   |   |   |   |   |   |   |   |   |    |    |    |    |    |
| <i>Caheniasaccites flavatus</i>       |   |   | P | P | P | P | P |   |   |    |    |    |    |    |
| <i>Potonieisporites lelei</i>         |   |   | P | P | P | P | P | P | P | P  |    | P  | P  | P  |
| <i>Potonieisporites neglectus</i>     |   |   | P | P | P | P | P | P | P | P  | P  | P  | P  | P  |
| <i>Potonieisporites congoensis</i>    |   |   | P | P | P | P | P | P | P | P  | P  |    | P  | P  |
| <i>Potonieisporites novicus</i>       | P |   | P | P | P | P | P | P | P | P  | P  | P  | P  | P  |
| <i>Limistisporites rectus</i>         |   |   |   |   |   |   |   | P |   | P  |    |    |    |    |
| <i>Scheuringipollenites maximus</i>   | P |   |   |   |   |   |   |   |   |    |    |    |    |    |


  
 Increase in palynodiversity correlatable to-  
 Warm temperate Biome 6 of Walter (1985)
 
 Low palynodiversity correlatable to-  
 Cold temperate Biome 8 of Walter (1985)

recognized three more or less distinct zones of a sandur surface related to distance from the ice margin- proximal, intermediate and distal zone, with corresponding decreases in the mean sediment size on the surface of most aggrading sandur. Hence, deposition in distal reaches of the outwash plain is envisaged for phase I based on fine clastic material. Alternatively, deposition in a kettle hole/lake could be proposed, which are depressions formed by blocks of ice that are detached from a receding glacier and their eventual melting (Smith, 1985). The absolute abundance of AOM (90%, Fig. 4 and 5) in palynofacies I suggests prevalence of anoxic conditions during deposition. The colourless spongy to granulate AOM masses bearing a mild fluorescence and the presence of *Botryococcus* confirmed their algal nature (Tyson, 1995; Martínez et al., 2008). Presence of pollen and scarce spores agree with their deposition far from vegetated upland areas where pollen delivery is primarily by air transport in the absence of river inputs (Farley, 1988; Tyson, 1995; Falcon-Lang et al., 2004). A poor and low diverse vegetation during this phase is also reflected by paucity in phytoclasts (Figs. 3 and 4) and low TOC (0.5-0.6%) and higher negative  $\delta^{13}\text{C}$  (-24.9 ‰) values (Fig. 6A and B).

#### Mid Interglacial Phase

This phase reflects amelioration of climate during which active

channel systems sweeping across the outwash plain developed and there was a slow stabilization of vegetation. Hence, more stable paleoclimatic conditions triggered an increase in the diversity of the floras, revealed by the palynofloral composition (see Table 1). However, the predominance of xerophilous conifers (Fig. 3), along with seasonally controlled vegetation composed of meso-hygrophilous cordaitaleans and pteridosperms and ferns from lowlands outside paleovalleys, and rare hygrophilous lycopsids in refugia or in riparian niches (Falcon-Lang et al., 2004) support a paleoclimate under cool and less humid conditions. The cordaitaleans are closely related to the conifers with which they were initially thought to be as strictly “upland” dominant para-autochthonous elements in intraformational channel fill (Feldman et al., 2005; Hilton and Bateman 2006; Falcon-Lang et al., 2009). However, they were also frequently encountered in basal lowlands (DiMichelle et al., 2010) preferring a range of habitats such as peat-forming and clastic wetlands, seasonally-dry settings, well-drained floodplains and drought-prone habitats (Falcon-Lang and Bashforth, 2005) in association with pteridosperms, few calamitaleans, and sigillarian lycopsids, in the tropical Euramerican landscapes (Falcon-Lang 2003; Falcon-Lang et al., 2004; Šimůnek, 2008). Collectively, there is an increase of vegetation in this phase, seasonally controlled. Deposition in distal dysoxic to sub-oxic conditions is

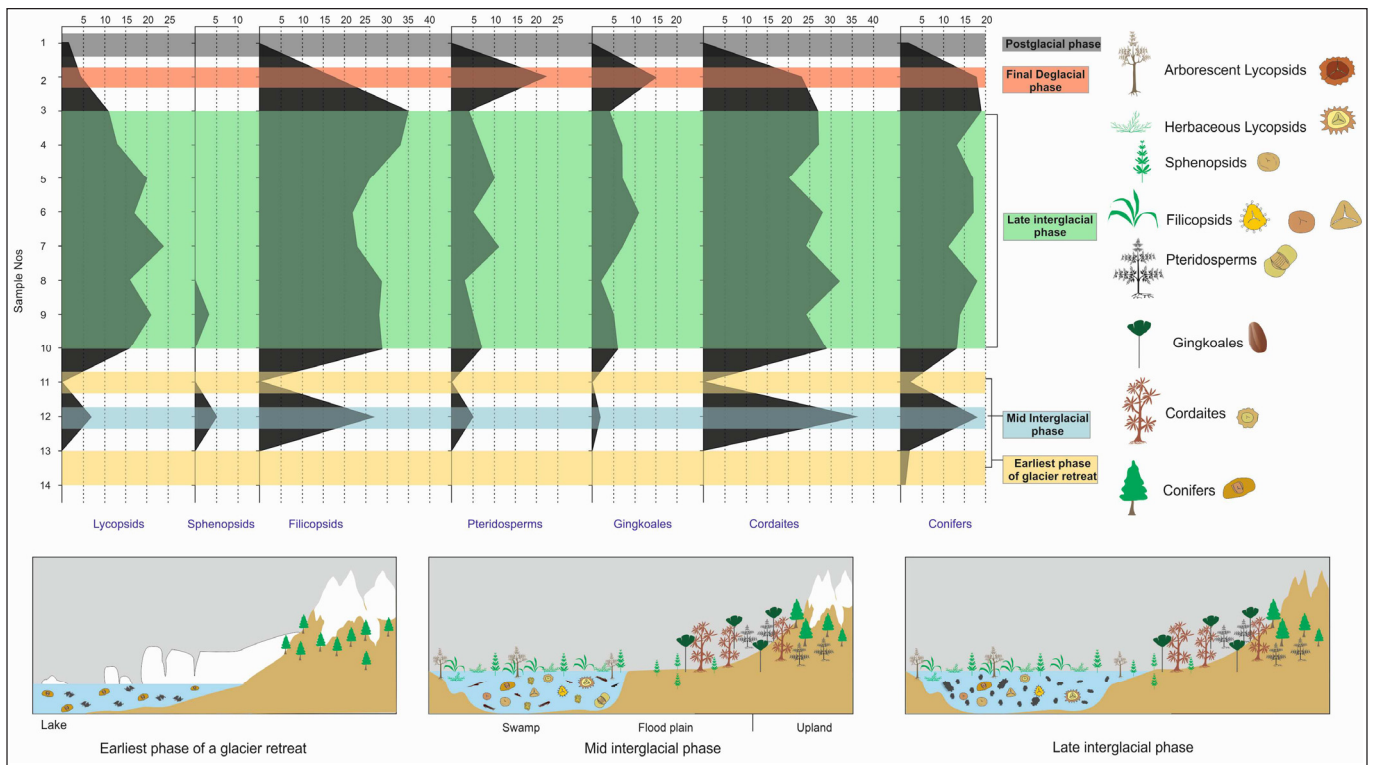


**Fig. 3.** Relative abundance of the plant groups documented in MAWP 114 Borehole that characterizes five paleoenvironmental stages in the studied area.

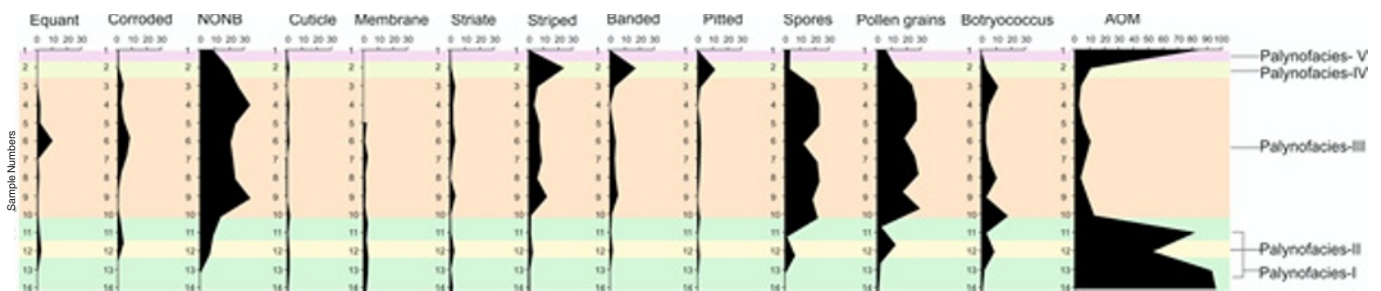


**Fig. 4.** Distribution of the palynofacies components and demarcation of I-V palynofacies along MAWP 114 Borehole.

inferred based on dominance of AOM with low to moderate palynomorphs. The above inference and a higher frequency of AOM and *Botryococcus* and low phytoclasts as part of the palynofacies II (Fig. 4) are also supported by a less negative  $\delta^{13}\text{C}$  (-22 ‰) and a low TOC value (c. 0.5%) (Fig. 6A and B).

**Late Interglacial Phase**

This phase corresponds to the palynofacies III which is most dominant in the studied interval characterized by the reduction in AOM (3-12%) and an increase in palynomorphs (38-70%) and subdominance of phytoclasts (18-53%). It witnessed delta-plain progradation as the main landscape, with mineral-substrates and stabilization of high-diverse vegetation under seasonal conditions. Drier habitats include a broad range of poorly drained floodplains and levees mainly represented by allochthonous and para-autochthonous conifers, cordaitaleans and pteridosperms, whereas wetland habitats are represented by swamps to riparian and fluvio-deltaic environments containing lycopsiids, cordaitaleans, pteridosperms, and ferns (Fig. 3).

Into this landscape, deposition of palynomorphs and phytoclasts occurred mainly in distal parts of marshy wetlands containing fine clastic and peaty material or in inactive areas of outwash fans and other fresh water bodies. Most of the opaque and especially wood

(xylem) that are quite abundant in several samples of this palynofacies are derived from the highly lignified mechanical support tissue of higher plants. As lignin is highly resistant to decay, it tends to become selectively preserved and therefore, concentrated in sub-oxic facies rather than fully anoxic conditions (Tyson, 1995). A median proximal to distal sub-oxic to oxic environment of deposition can be envisaged for palynofacies III. This is also supported by some fluctuations in both  $\delta^{13}\text{C}$  ranging between ~ -22‰ - 21‰ and TOC values (Fig. 6A and B) reflecting variations in redox conditions at the time of deposition. Therefore, the increase in palynodiversity is correlatable with the shift from arid conditions prevailing in the lower phases to humid and temperate climate conditions equivalent to modern Warm temperate Biome 6 of Walter (1985).

**Final Deglacial Phase**

The rising temperatures led to the melting of glaciers triggering eustatic sea level rise and changes in sedimentary transport processes, weathering and expansion of vegetation.

This phase characterized by palynofacies IV, exhibits subdominance of conifer and cordaitean pollen grains (Fig. 3) recording their signature of upland floras that survived the deglaciation-driven flooding of lowland environments (Falcon-Lang and Bashforth, 2004).

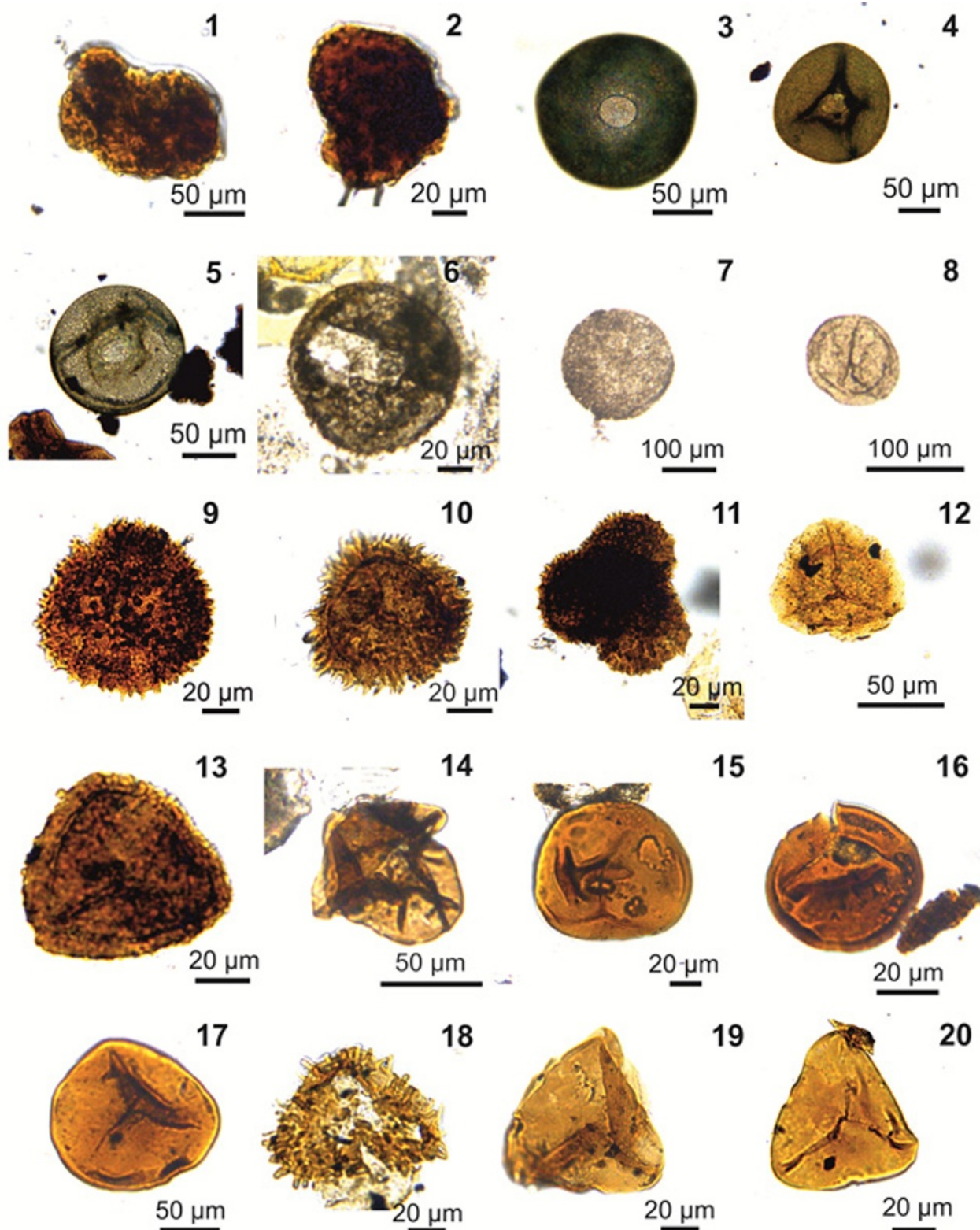
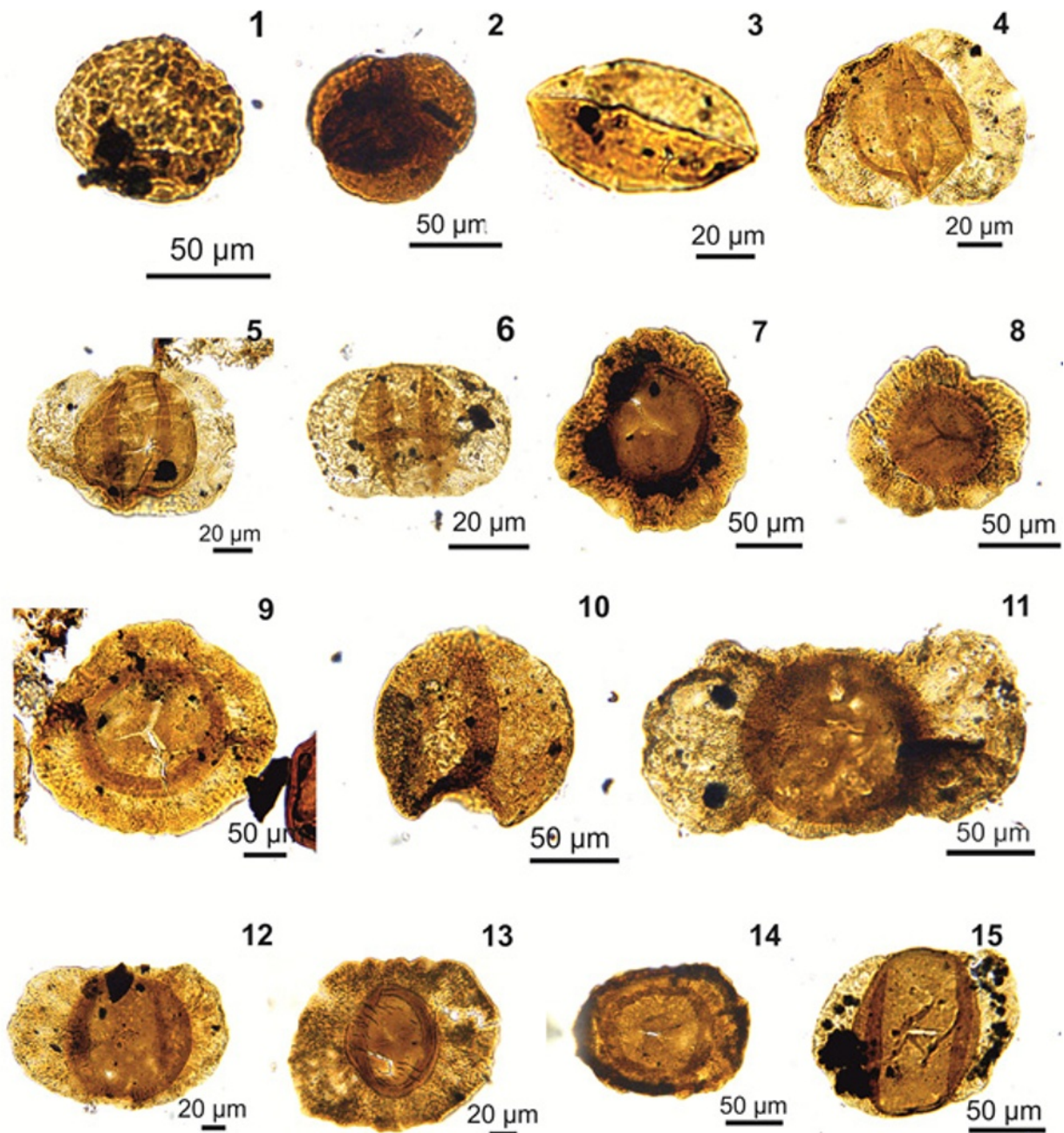


**Plate 1.** Some spores from the study area. 1, 2. *Botryococcus braunii* Kützing. 1. BSIP 16729, EF: Z.36.2; 2. BSIP 16729, EF: Y.52.1. 3-6. *Thoecamoebia* sp. 3. BSIP 16725, EF: X.53; 4. BSIP 16739, EF: Q.57; 5. BSIP 16737, EF: Q.34; 6. BSIP 16728, EF: P.45. 7. Unknown sp. BSIP 16728, EF: E.52.3. 8. Unknown sp. BSIP 16725, EF: Y.66.1. 9. *Cristatisporites conatus* (Lele and Makada) Kavali, Roy, di Pasquo, Puttojirao, Sharma, Kumar. BSIP 16732, EF: K.45. 10. *Cristatisporites pseudozonatus* (Lele and Makada) Jones & Truswell. BSIP 16732, T. 39.4. 11. *Cristatisporites* tetrad. BSIP 16732, EF: W.44.3. 12. *Indotriadites korbaensis* Tiwari 1964 BSIP 16738, EF: O.34.1 13. *Lundbladispora* sp. BSIP 16731, EF: T.39.1. 14. *Calamospora hartungiana* Schopf, Wilson and Bentall. BSIP 16732, EF: T.39.4. 15-17. *Punctatisporites gretensis* Balme and Hennelly. 15. BSIP 16731, EF: W.85. 16. BSIP 16731, EF: X.46. 17. BSIP 16731, EF: T.39.1. 18. *Horriditriletes ramosus* (Balme and Hennelly, 1956) Bharadwaj & Salujha. BSIP 16731, EF: X.52.1. 19. *Leiotriletes directus* Balme and Hennelly. BSIP 16732, EF: V.60. 20. *Leiotriletes virkkii* Tiwari. BSIP 16732, EF: V. 60.



**Selected pollen grains from the study area:** 1. *Verrucosiporites verrucosus* (Ibrahim) Ibrahim. BSIP 16735, EF: V.39.4. 2. *Verrucosiporites* sp. tetrad. BSIP 16735, EF: R.50. 3. *Cycadopites cymbatus* Balme and Hennelly. BSIP 16731, EF: V.52. 4. *Protohaploxypinus pennatulus* (Andreyeva) Hart. BSIP 16732, EF: U.24.2 5,6. *Protohaploxypinus limpidae* (Balme and Hennelly) Balme and Playford. 5. BSIP 16732, EF: Q.57.3; 6. BSIP 16732, EF: S.33.1. 7. *Cannanoropollis janakii* Potonié and Sah. 7. BSIP 16736, EF: S.63.1; 8. *Cannanoropollis densus* BSIP 16735, EF: V.39.4. 9. *Plicatipollenites malabarensis* (Potonié and Sah) Foster. BSIP 16732, EF: S.41 10. *Scheuringipollenites maximus* (Hart) Tiwari. BSIP 16739, EF: S.34.1. 11. *Caheniasaccites flavatus* (Bose and Kar) Azcuy and di Pasquo. BSIP 16734, EF: S.49. 12. *Potonieisporites lelei* Maheshwari. BSIP 16732, EF: P.28. 13. *Potonieisporites novicus* (Bharadwaj) Poort and Veld. BSIP 16730, EF: Y.42. 14. *Potonieisporites congoensis* Bose and Maheshwari. BSIP 16726, EF: L. 54.1. 15. *Limitisporites rectus* Leschik. BSIP 16735, EF: T.51

The palynodiversity reflects a higher proportion of allochthonous extrabasinal elements coming from intramontane positions through rivers to relative lowlands in distal areas during climatically wetter periods of peat formation. It is inferred that air transport of pollen grains into the area of deposition reflect a wider distribution of gymnosperms from upland to lowlands and can be combined with stronger wind circulation across the Palaeotethys (Saltzman 2003; Shi and Waterhouse 2010; Heavens et al., 2015).

#### Post Glacial Phase

The complete withdrawal of glaciers led to basin uplift and exhumation due to post glacial isostatic rebound, which led to the

development of normal faults leading to the deposition of fluvial deposits of post Talchir, Karharbari / Barakar Formation (Bhattacharya et al., 2005; Bhattacharya and Bhattacharya, 2015).

The sparse floral record and higher AOM of terrestrial nature (sample 1, Figs. 3-5) and lower TOC values (Fig. 6B) of this phase are likely due to taphonomic processes during deposition of fine to medium grained sandstones under distal dysoxic to anoxic conditions. Nevertheless, it is not believed that there was a reduction in the diversity and abundance of the floras considering the general abundance of the coal precursor plant communities present in upper Talchir palynoaemblages (Table 2), which is also consistent with the record of overlying relatively thin (1–90 cm) numerous coal intervals in the

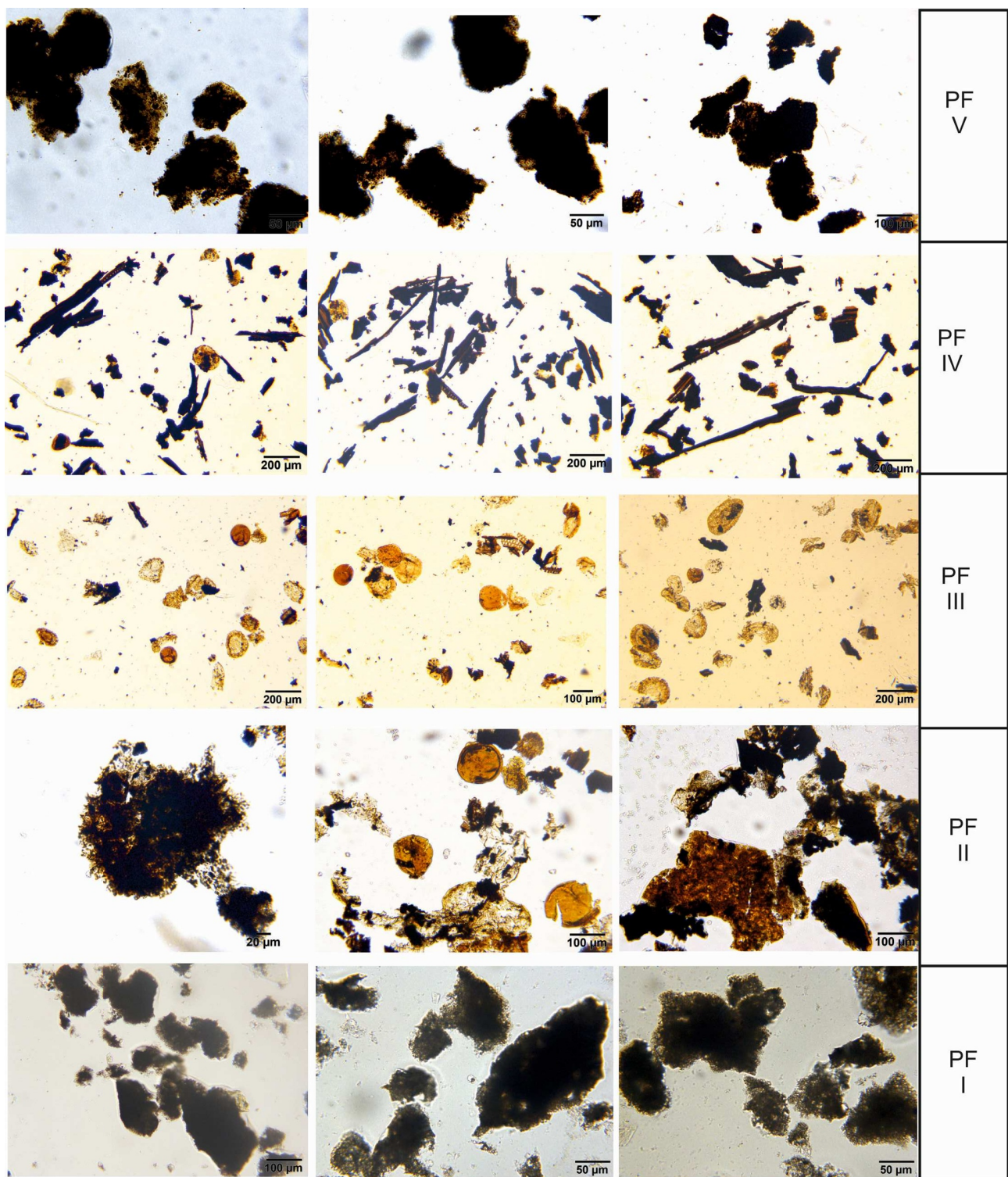


Fig. 5. Kerogen aspect of palynofacies type I-V . For relative abundance of each component see Figure 4.

Barakar Formation. Unfortunately, mine officers did not allow sampling the coal levels observed above the sandstone bed and the remaining core upwards. The coal intervals prove the establishment of short lived mires in emergent delta-top environments under low subsidence rates, which would favour the formation of peat and their eventual transformation into coal in this region as well as in other Indian basins (Bhattacharya et al., 2005; Mukhopadhyay et al., 2010; Bhattacharya and Bhattacharya, 2015 and references therein).

Therefore, considering the detailed palaeoenvironmental changes based on palynofacies and floristic composition and geochemical data obtained from a thin shale core of the Talchir and the lower fine

sandstone layer of the Barakar formations, a correlation to climatic belts of Scotese et al., (2021) is proposed.

During the lower two phases, sub-polar climate related to cold-arid conditions prevailed (Fig. 3) and vegetation could have been similar to modern Cold temperate Biome 8 of Walter (1985) (Table 1). The Late interglacial (III) to postglacial (IV-V) phases (Fig. 3) could be correlated to Biome 6 of Walter (1985) (Table 1) and would correspond to the “seasonally warm/cold temperate” of the modern Köppen Climate Belts (Scotese et al., 2021), based on palynofacies and more diverse floristic composition reinforced by geochemical data (Fig. 6A and B). As described above, the last phase identified just



**Table 2.** Alphabetical list of Spores and pollen documented in the lower (LT) and upper (UT) Talchir Formation of India. References: A= Present study; B= Wardha Basin (Lele, 1979; Kavali et al., 2021); C= Godavari Basin (Tiwari and Tripathi, 1988, 1992; Tiwari, 1994; Jha et al., 2018; Aggarwal and Jha, 2013); D= Satpura Basin (Tiwari and Tripathi, 1988, 1992; Tiwari, 1994); E= Son Mahanadi Basin (Tiwari and Tripathi, 1988, 1992; Tiwari 1994); F= Damodar Basin (Tiwari and Tripathi, 1988, 1992; Tiwari 1994); G= Rajmahal Basin (Tiwari 1994; Murthy et al., 2020)(Note: Since they have been reported extensively from all the basins, only those publications which summarize data from different basins have been referred).

| Taxa                                      | Basin | A  |    | B  |    | C  |    | D  |    | E  |    | F  |    | G  |    |
|---|-------|----|----|----|----|----|----|----|----|----|----|----|----|----|----|
|   |       | LT | UT | LT | UT | LT | UT | LT | UT | LT | UT | LT | UT | LT | UT |
| <i>Brevitriletes cornutus</i>             |       |    | X  |    | X  |    | X  |    | X  |    | X  |    | X  |    | X  |
| <i>Cahenisaccites flavatus</i>            |       |    | X  |    | X  |    | X  |    | X  |    | X  |    | X  |    | X  |
| <i>Calamospora hartungiana</i>            |       |    | X  |    | X  |    | X  |    | X  |    | X  |    |    |    |    |
| <i>Calamospora landiana</i>               |       |    |    |    | X  |    | X  |    | X  |    | X  |    | X  |    |    |
| <i>Calamospora liquida</i>                |       |    |    |    | X  |    | X  |    | X  |    | X  |    | X  |    | X  |
| <i>Cannanoropollis densus</i>             |       | X  |    | X  | X  | X  | X  | X  | X  | X  | X  | X  | X  | X  | X  |
| <i>Canannaropollis janakii</i>            |       | X  | X  | X  | X  | X  | X  | X  | X  | X  | X  | X  | X  | X  | X  |
| <i>Cannanoropollis mehtae</i>             |       |    |    | X  | X  | X  | X  | X  | X  | X  | X  | X  | X  |    |    |
| <i>Cannanoropollis triangularis</i>       |       | X  | X  | X  | X  | X  | X  | X  | X  | X  | X  | X  | X  | X  | X  |
| <i>Circumplicatipollis stigmatus</i>      |       |    |    |    |    |    |    |    |    |    |    |    |    | X  | X  |
| <i>Concavissimisporites grumulus</i>      |       |    |    |    | X  |    |    |    |    |    |    |    |    |    |    |
| <i>Converrucosisporites confluens</i>     |       |    |    |    | X  |    |    |    |    |    |    |    |    |    |    |
| <i>Converrucosisporites micronodosus</i>  |       |    |    |    | X  |    |    |    |    |    |    |    |    |    |    |
| <i>Convolutispora ordonensis</i>          |       |    |    |    | X  |    |    |    |    |    |    |    |    |    |    |
| <i>Costatacycclus crenatus</i>            |       |    |    |    | X  |    |    |    |    |    |    |    |    | X  | X  |
| <i>Cristatisporites conatus</i>           |       | X  |    | X  | X  |    | X  |    | X  |    | X  |    | X  |    | X  |
| <i>Cristatisporites pseudozonatus</i>     |       | X  |    | X  | X  |    | X  |    | X  |    | X  |    | X  |    | X  |
| <i>Cycadopites cymbatus</i>               |       | X  |    | X  | X  |    | X  |    | X  |    | X  |    | X  |    | X  |
| <i>Cyclogranisporites gondwanensis</i>    |       |    |    |    | X  |    | X  |    | X  |    | X  |    | X  |    |    |
| <i>Divarisaccus lelei</i>                 |       |    |    |    | X  |    | X  |    | X  |    | X  |    | X  | X  | X  |
| <i>Divarisaccus strengeri</i>             |       |    |    |    |    |    |    |    |    |    |    |    | X  | X  | X  |
| <i>Gondwanapollis cf. frenguelli</i>      |       |    |    |    |    |    |    |    |    |    |    |    |    | X  |    |
| <i>Granulatisporites austroamericanus</i> |       |    |    |    | X  |    | X  |    | X  |    | X  |    | X  |    | X  |
| <i>Horriditriletes gondwanensis</i>       |       | X  |    | X  | X  |    | X  |    | X  |    | X  |    | X  |    | X  |
| <i>Horriditriletes ramosus</i>            |       | X  |    | X  | X  |    | X  |    | X  |    | X  |    | X  |    | X  |
| <i>Horriditriletes uruguaiensis</i>       |       |    |    |    | X  |    |    |    |    |    |    |    |    |    |    |
| <i>Illinites talchirensis</i>             |       |    |    |    | X  |    | X  |    | X  |    | X  |    | X  |    | X  |
| <i>Latusipollenites quadrisaccatus</i>    |       |    |    |    | X  |    |    |    |    |    |    |    |    |    |    |
| <i>Leiotriletes directus</i>              |       | X  |    | X  | X  |    | X  |    | X  |    | X  |    | X  |    | X  |
| <i>Leiotriletes virkki</i>                |       | X  |    | X  | X  |    | X  |    | X  |    | X  |    | X  |    |    |
| <i>Limitisporites hexagonalis</i>         |       | X  |    | X  | X  |    | X  |    | X  |    | X  |    | X  |    | X  |
| <i>Limitisporites rectus</i>              |       |    |    |    | X  |    | X  |    | X  |    | X  |    | X  |    | X  |
| <i>Lunatisporites noviaulensis</i>        |       |    |    |    | X  |    | X  |    | X  |    | X  |    | X  |    | X  |
| <i>Lunatisporites varisectus</i>          |       |    |    |    | X  |    | X  |    | X  |    | X  |    | X  |    | X  |
| <i>Lunbladispora sp.</i>                  |       | X  |    |    |    |    |    |    |    |    |    |    |    |    |    |
| <i>Marsupipollenites triradiatus</i>      |       |    |    |    | X  |    | X  |    | X  |    | X  |    | X  |    |    |
| <i>Marsupipollenites striatus</i>         |       |    |    |    | X  |    | X  |    | X  |    | X  |    | X  |    |    |
| <i>Microbaculispora tentula</i>           |       |    |    |    | X  |    | X  |    | X  |    | X  |    | X  |    | X  |
| <i>Pakhapites fusus</i>                   |       |    |    |    | X  |    |    |    |    |    |    |    |    |    |    |
| <i>Plicatipollenites gondwanensis</i>     |       | X  |    | X  | X  | X  | X  | X  | X  | X  | X  | X  | X  | X  | X  |
| <i>Plicatipollenites malabarensis</i>     |       | X  |    | X  | X  | X  | X  | X  | X  | X  | X  | X  | X  | X  | X  |
| <i>Plicatipollenites trigonalis</i>       |       | X  |    | X  | X  | X  | X  | X  | X  | X  | X  | X  | X  | X  | X  |
| <i>Potonieisporites barreli</i>           |       |    |    |    | X  | X  | X  | X  | X  | X  | X  | X  | X  | X  | X  |
| <i>Potonieisporites congoensis</i>        | X     | X  |    | X  |    | X  | X  | X  | X  | X  | X  | X  | X  | X  | X  |
| <i>Potonieisporites densus</i>            |       |    |    |    | X  |    | X  |    | X  |    | X  |    | X  |    |    |
| <i>Potonieisporites lelei</i>             | X     | X  |    | X  | X  | X  | X  | X  | X  | X  | X  | X  | X  | X  | X  |
| <i>Potonieisporites magnus</i>            |       |    |    |    | X  | X  | X  | X  | X  | X  | X  | X  | X  | X  | X  |
| <i>Potonieisporites neglectus</i>         | X     | X  | X  | X  | X  | X  | X  | X  | X  | X  | X  | X  | X  | X  | X  |
| <i>Potonieisporites novicus</i>           | X     | X  |    | X  | X  | X  | X  | X  | X  | X  | X  | X  | X  | X  | X  |
| <i>Protohaploxylinus latissimus</i>       |       |    |    |    | X  |    | X  |    | X  |    | X  |    | X  |    |    |
| <i>Protohaploxylinus limpidus</i>         |       | X  |    | X  |    | X  |    | X  |    | X  |    | X  |    |    |    |
| <i>Protohaploxylinus pennatulus</i>       |       | X  |    |    |    |    |    |    |    |    |    |    | X  |    |    |
| <i>Protohaploxylinus perfectus</i>        |       |    |    |    | X  |    | X  |    |    |    | X  |    | X  |    | X  |
| <i>Punctatisporites fungosus</i>          |       | X  |    | X  |    | X  |    | X  |    | X  |    | X  |    | X  | X  |
| <i>Punctatisporites gretensis</i>         | X     | X  |    | X  |    | X  |    | X  |    | X  |    | X  |    | X  | X  |
| <i>Scheurngipollenites maximus</i>        |       |    |    |    | X  |    |    |    |    |    |    |    |    |    | X  |
| <i>Stellapollenites talchirensis</i>      |       |    |    |    | X  |    | X  |    | X  |    | X  |    | X  |    | X  |
| <i>Striatoabietites multistriatus</i>     |       |    |    |    | X  |    |    |    |    |    |    |    |    |    |    |
| <i>Tuberisaccites lobatus</i>             |       |    |    |    |    | X  | X  | X  | X  | X  | X  | X  | X  | X  | X  |
| <i>Verrucosisporites andersonii</i>       |       |    |    |    | X  |    |    |    |    |    |    | X  | X  |    |    |
| <i>Verrucosisporites verrucosus</i>       |       | X  |    | X  |    | X  |    | X  |    | X  |    | X  |    |    |    |
| <i>Vesicaspora sp.</i>                    |       |    |    |    |    |    |    |    |    |    |    |    |    |    | X  |
| <i>Vittatina subsaccata</i>               |       | X  |    | X  |    |    |    |    |    |    |    |    |    |    |    |
| <i>Vittatina vittifera</i>                |       |    |    |    | X  |    |    |    |    |    |    |    |    |    |    |

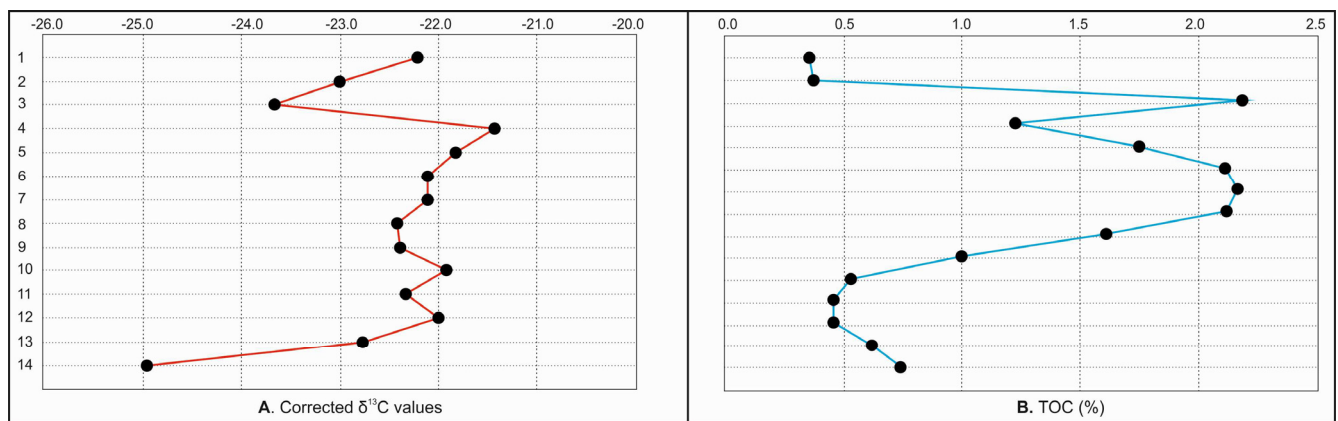


**Fig. 6A.** Results from Carbon isotope ( $\delta^{13}\text{C}$ ) analysis (‰; VPDB). **B.** Total Organic Carbon (TOC) values of samples 1-14 from the studied borehole MAWP 114..

before the first record of coal beds of the Barakar Formation confirms a paleoclimatic warming trend. The modern warm temperate Biome 6 of Walter (1985) is suitable for comparing the floristic features during these three phases despite the differences between modern paleogeographic configuration of Southern Hemisphere, which is mostly dominated by oceans with smaller and separated continents.

In summary, an overall palaeoclimatic change throughout this section testifies a shift from Late Pennsylvanian Gzhelian (~302) cold-temperate-arid (Boucot et al., 2013) to Asselian (~297, early Permian) temperate-humid climatic conditions (Scotese et al., 2021).

## CONCLUSIONS

Late Paleozoic climate change had pronounced effects on vegetation wherein major palaeoecological changes were exhibited in the relative abundance of taxa due to postglacial climatic warming.

Quantitative counts of relative abundance of palynofacies components and botanical affinities of palynomorphs and geochemical data (TOC and  $\delta^{13}\text{C}$ ) obtained from fourteen shale and one sandstone interval from borehole MAWP 114, allowed us to assess late Pennsylvanian-early Permian vegetational communities in a high-latitude, intracratonic setting of India. A total of 29 palynotaxa were documented, comprising 13 trilete spores derived from lycophytes and monilophytes (pteridophytes and sphenophytes) and 16 monosaccate and bisaccate pollen grains of gymnosperm groups (Cordaitalean, Coniferalean, Ginkgo/Cycadalean, Pteridosperms). Algal remains mostly *Botryococcus* are also variably present.

A relationship between global climatic change and vegetation in the aftermath of the late Paleozoic ice age is suggested, and five phases delimited: (I) earliest phase of a glacier retreat; (II) mid interglacial phase; (III) late interglacial phase; (IV) final deglacial phase; (V) postglacial phase. Hence, plant assemblages and palynofacies features of the Talchir Formation demonstrate that late Pennsylvanian and early Permian temperate vegetation contracted and expanded in response to glacial-interglacial rhythms.

In the lower part of the section, a cold-arid climate persisted wherein a primitive conifer community developed on the surrounding uplands. This vegetation is similar to modern Cold temperate Biome 8 of Walter (1985). There is also evidence that a specialised autochthonous freshwater algal *Botryococcus* occupied small ponds in lowland wetland environments.

In the upper part of the section more diverse vegetation developed under temperate-humid conditions equivalent to modern Warm temperate Biome 6 of Walter (1985), wherein a cycad-like and lycopsid vegetation developed in the lowland alluvial plains. Striate and non - striate bisaccate pollen producing gymnospermous flora developed in the uplands or in better drained areas.

These climatic and biotic shifts documented in the studied samples

of the Talchir Formation are supported by coeval palynofloras across India, testifying similar climate fluctuations around Gondwana.

*Acknowledgements:* The authors are grateful to V. Prasad, Director of the Birbal Sahni Institute of Palaeosciences, for granting permission to publish this article ((BSIP/RDCC no.76). PSK is thankful to the authorities of CMPDI for allowing them to carry out fieldwork and to A. Saxena, Regional Director CMPDI in Nagpur, for providing samples and assistance in the field. MDP is grateful to CICYTTP-CONICET-ER-UADER (Entre Ríos, Argentina) for permitting to collaborate in this work supported by research grants PIP CONICET 0812 (Argentina). We are grateful to Dr. Agrawal S for helping in isotope analysis. We thank Technical staff S. Srivastava for preparing the slides. This work was funded by the Birbal Sahni Institute of Palaeosciences (BSIP/RDCC no.76), an autonomous research Institute under the Department of Science and Technology, Government of India.

## References

- Acharyya, S. K. (2019a) Developments in structural Geology and tectonics. *In: Acharyya, S.K (Ed.), v. 4, pp.1–4. Amsterdam: Elsevier Academic Press.*
- Acharyya, S.K. (2019b) Developments of Gondwana basins in the Indian shield. *In: Acharyya, S.K (Ed.), Developments in structural Geology and tectonics. v. 4, pp.17–29. Amsterdam: Elsevier Academic Press.*
- Aggarwal, N., Jha, N. (2013) Permian palynostratigraphy and palaeoclimate of Lingala-Koyagudem coalbelt, Godavari Graben, Andhra Pradesh, India. *Jour. Asian Earth Sci., v.64, pp.38–57.*
- Agrawal, S., Srivastava, P., Meena, S.N.K., Rai, S.K., Bhushan, R., Misra, D.K., Gupta, A.K. (2015) Stable ( $\delta^{13}\text{C}$  and  $\delta^{15}\text{N}$ ) isotopes and magnetic susceptibility record of late holocene climate change from a lake profile of the northeast Himalaya. *Jour. Geol. Soc. India, v.86, pp.696–705.*
- Agrawal, S., Verma, P., Rao, M.R., Garg, R., Kapur, V.V., Bajpai, S. (2017) Lignite deposits of the Kutch basin, western India: carbon isotopic and palynological signatures of the early eocene hyperthermal event ETM2. *Jour. Asian Earth Sci., v.146, pp.296–303.*
- Archangelsky, S., Gamero, J.C. (1979) Palinología del Paleozoico Superior en el subsuelo de la Cuenca Chacoparanense, República Argentina. I. Estudio sistemático de los palinomorfos de tres perforaciones de la Provincia de Córdoba. *Revista Española de Micropaleontología, v.11, pp. 417–478.*
- Azcuy, C.L., Di Pasquo, M. (2000) Palynology of the Late Carboniferous from the Tarija Basin, Argentina: a systematic review of monosaccate pollen genera. *Palaeontographica, v.253, pp.103–137.*
- Backhouse, J. (1991) Permian palynostratigraphy of the Collie Basin, Western Australia. *Rev. Palaeobot. Palynol., v.67, pp.237–314.*
- Backhouse, J., Mory, A.J. (2020) Mid-Carboniferous – Lower Permian palynology and stratigraphy, Canning Basin, Western Australia. *Geol. Surv. Western Australia, Report, v.207, 133p.*
- Balme, B. E. (1970) Palynology of Permian and Triassic Strata in the Salt Range and Surghar Range, West Pakistan. *In: Kummel B., Teichert C. (eds.), Stratigraphic boundary problems: Permian and Triassic of West*

- Pakistan. Univ. Kansas, Spec. Publ., v.4, pp.305–453.
- Balme, B.E. (1995) Fossil *in situ* spores and pollen grains: an annotated catalogue. Rev. Palaeobot. Palynol., v.87, pp.81–323.
- Banerjee, I. (1966) Turbidities in a glacial sequence: A study from the Talchir Formation, Raniganj Coalfield. Jour. Geol., v.74(5P1), pp.593–606.
- Banerjee, M., D’Rozario, A. (1990) Palynostratigraphic correlation of Lower Gondwana Sediments in the Chuparbhita and Hura basins, Rajmahal Hills, Eastern India. Rev. Palaeobot. Palynol., v.65, pp.239–255.
- Beri, A., Blanco, X., Varela, L., di Pasquo, M., Souza, P.A. (2019) Sampling biases and Paleozoic sporomorphs diversity dynamics in Western Gondwana strata. Jour. South Amer. Earth Sci., v.98, pp.102457.
- Bernardes-de-Oliveira, M.E.C., Kavali, P.S., Mune, S.E., Shivanna, M., Souza, P.A., Iannuzzi, R., Jasper, A., Hoelzel, A., Boardman, D.R., Rohn, R., Ricardi-Branco, F. (2016) Pennsylvanian-early Cisuralian interglacial macrofloristic succession in Paraná Basin of the state of São Paulo. Jour. South Amer. Earth Sci., v.72, pp.351–374.
- Bhattacharya, B. (2003) Storm event beds in Talchir Formation, Jayanti Basin, Jharkhand, India. Indian Jour. Earth Sci., v.30(1–4), pp.37–41.
- Bhattacharya, B. (2013) Sedimentary cycles related to the Late Paleozoic cold-warm climate change, Talchir Formation, Talchir Basin, India. Earth Resour., v.1(1), pp.12–25.
- Bhattacharya, B., Bhattacharya, H.N. (2007) Implications of trace fossil assemblages from Late Paleozoic glaciomarine Talchir Formation, Raniganj Basin, India. Gondwana Res., v.12(4), pp.509–524.
- Bhattacharya, B., Bhattacharya, H.N. (2012) Implications of Mud-clast conglomerates within Late Paleozoic Talchir glaciomarine succession, Talchir Basin, India. Indian Jour. Geosci., v.66(1), pp.69–78.
- Bhattacharya, B., Bhattacharya, H.N. (2014) Late Paleozoic glaciation and post-glacial transgressions in eastern peninsular India: Extent and implications, *In*: 19<sup>th</sup> International Sedimentological Congress “Sedimentology at the Crossroads of New Frontiers” — Abstracts. 18–22 August 2014, Geneva, Switzerland, p.71.
- Bhattacharya, H.N., Bhattacharya, B. (2006) A Permo-Carboniferous tide-storm interactive system: Talchir Formation, Raniganj Basin, India. Jour. Asian Earth Sci., v.27(3), pp.303–311.
- Bhattacharya, H.N., Bhattacharya, B. (2010) Soft-sediment deformation structures from an ice-marginal storm-tide interactive system, Permo-Carboniferous Talchir Formation, Talchir Coal basin, India. Sediment. Geol., v.223(3–4), pp.380–389.
- Bhattacharya, H.N., Bhattacharya, B. (2011) Sole marks in storm beds from a glacially influenced Late Paleozoic shallow sea, Talchir Formation, Talchir Basin, India. Indian Jour. Geosci., v.65(3), pp.175–188.
- Bhattacharya, H.N., Bhattacharya, B. (2015) Lithofacies architecture and palaeogeography of the Late Paleozoic glaciomarine Talchir Formation, Raniganj Basin, India. Jour. Palaeogeog., v.4(3), pp.269–283.
- Bhattacharya, H.N., Bhattacharya, B., Chakraborty, A. (2009) Architecture of storm event beds from Late Paleozoic glaciomarine Talchir Formation, Talchir Coalfield, Orissa. Vistas in Geol. Res., v.8, pp.1–10.
- Bhattacharya, H.N., Bhattacharya, B., Chakraborty, I., Chakraborty, A. (2004) Sole marks in storm event beds in the Permo-Carboniferous Talchir Formation, Raniganj Basin, India. Sediment. Geol., v.166(3–4), pp.209–222.
- Bhattacharya, H.N., Chakraborty, A., Bhattacharya, B. (2005) Significance of transition between Talchir Formation and Karharbari Formation in Lower Gondwana basin evolution — A study in West Bokaro Coal Basin, Jharkhand, India. Jour. Earth Syst. Sci., v.114(3), pp.275–286.
- Bhattacharya, H.N., Goswami, A., Chakraborty, A. (2002) Sedimentary facies analysis of a Permo-Carboniferous terminoglacial succession, Saharjuri Basin, Jharkhand. Jour. Geol. Soc. India, v.60(4), pp.401–410.
- Blanford, W.T., Blanford, H.F., Theobald, W. (1856) On the geological structure and relations of the Talchir Coalfield in the district of Cuttack. Geol. Surv. India Mem., v.1, pp.1–98.
- Bose, P.K., Mukhopadhyay, G., Bhattacharyya, H.N. (1992) Glaciogenic coarse clastics in a Permo-Carboniferous bedrock trough in India: A sedimentary model. Sediment. Geol., v.76 (1–2), pp.79–97.
- Boucot, A.J., Chen, X., Scotese, C.R. (2013) Phanerozoic paleoclimate: An atlas of lithologic indicators of climate. SEPM Concepts in Sedimentology and Paleontology, No.11, 478p. Tulsa.
- Chakraborty, A., Bhattacharya, H.N. (2005) Ichnology of a Late Paleozoic (Permo-carboniferous) glaciomarine deltaic environment, Talchir Formation, Saharjuri Basin, India. Ichnos, v.12(1), pp.31–45.
- Di Pasquo, M., Anderson, H., Isaacson, P. (2017) Record of a Pennsylvanian Cisuralian marine transgression, southern Bolivia: A short-lived event in western Gondwana? Palaeogeog., Palaeoclimat., Palaeoec., v.485, pp.30–45.
- Di Pasquo, M., Grader G. (2012) Palynology and paleoenvironment of the Asselian? Artinskian Copacabana Formation at Apillapampa near Cochabamba, Bolivia. Palynology, v.36, pp.264–276.
- Di Pasquo, M., Kavali, P.S., Dino, R., Shivanna, M., Bernardes-De-Oliveira, M.E.C., Roy, A. (2021) *Faunipollenites* Bharadwaj 1962 and *Protohaploxypinus* Samoilovich 1953 emend. Morbey 1975: morphologic comparison of oxidized and non- oxidized specimens from India and Brazil, and its taxonomic importance. Anais da Academia Brasileira de Ciencias, v.93(1), pp.1–25.
- DiMichele, W.A., Cecil, C.B., Montañez, I.P., Falcon-Lang, H.J. (2010) Cyclic changes in Pennsylvanian paleoclimate and effects on floristic dynamics in tropical Pangaea. Internat. Jour. Coal Geol., v.83, pp.329–344.
- DiMichele, W.A., Stein, W.E., Bateman, R.M. (2001) Ecological sorting during the Paleozoic radiation of vascular plant classes. *In*: Allmon, W.D., Bottjer, D.J. (Eds.), Evolutionary Paleocology. (pp. 285–335). Columbia University Press, New York.
- Dimitrova, T.K., Cleal, C.J. (2007) Palynological evidence for late Westphalian-early Stephanian vegetation change in the Dobrudzha Coalfield, NE Bulgaria. Geol. Mag., v.144, pp.513–524.
- Falcon-Lang, H.J. (2003) Anatomically preserved cordaitalean trees from a dryland alluvial plain setting, Joggins, Nova Scotia. Atlantic Geol., v.39, pp.259–265.
- Falcon-Lang, H.J. (2004) Pennsylvanian tropical rain forests responded to glacial-interglacial rhythms. Geology, v.32, pp.689–692.
- Falcon-Lang, H. J., Bashforth, A. R. (2005) Morphology, anatomy, and upland ecology of large cordaitalean trees from the Middle Pennsylvanian of Newfoundland. Rev. Palaeobot. Palynol., v.135, pp.223–243.
- Falcon-Lang, H.J., Nelson, W.J., Elrick, S., Looy, C.V., Ames, P.R., DiMichele, W.A. (2009) Incised channel fills containing conifers indicate that seasonally dry vegetation dominated Pennsylvanian tropical lowlands. Geology, v.37, pp.923–926.
- Falcon-Lang, H.J., Rygel, M.C., Calder, J.H., Gibling, M.R. (2004) An early Pennsylvanian waterhole deposit and its fossil biota in a dryland alluvial plain setting, Joggins, Nova Scotia. Jour. Geol. Soc. London, v.161, pp.209–222.
- Farley, M.B. (1988) Environmental variation, palynofloras, and paleoecological interpretation. *In*: DiMichele, W.A., Wing, S.L. (Eds.), Methods and Applications of Plant Paleocology, Paleontological Soc. Spec. Publ., v.3, pp.126–146.
- Feldman, H.R., Franseen, E.K., Joeckel, R.M., Heckel, P.H. (2005) Impact of longer-term modest climate shifts on architecture of high-frequency sequences (cyclothems), Pennsylvanian of Midcontinent, U.S.A. Jour. Sediment. Res., v.75, pp.350–368.
- Foster, C.B. (1979) Permian plant microfossils of the Blair Athol Coal Measures, Baralaba Coal Measures, and Basal Rewan Formation of Queensland. Geol. Surv. Queensland, v.372, pp.1–154.
- Ghosh, P.K., Mitra, N.D. (1975) History of Talchir sedimentation in Damodar valley basins. Mem. Geol. Surv. India, v.105, pp.1–117.
- Heavens, N.G., Mahowald, N.M., Soreghan, G.S., Soreghan, M.J., Shields, C.A. (2015) A model-based evaluation of tropical climate in Pangaea during the late Palaeozoic icehouse. Palaeogeog. Palaeoclimat. Palaeoec., v.425, pp.109–127.
- Hilton, J., Bateman, R.M. (2006) Pteridosperms are the backbone of seed-plant phylogeny. Jour. Torrey Botanical Soc., v.133, pp.119–168.
- Iannuzzi, R. (2013) The Carboniferous-Permian floral transition in the Paraná Basin. *In*: Lucas, S.G. (Ed.), The Carboniferous-Permian Transition. New Mexico Museum of Natural History and Science Bull., v.60, pp.132–136.
- Jensen, E.S. (1991) Evaluation of automated analysis of 15N and total N in plant material and soil. Plant Soil, v.133, pp.83–92.
- Jha, N., Aggarwal, N., Mishra, S. (2018) A review of the palynostratigraphy of Gondwana sediments from Godavari graben, India: global comparison and correlation of the Permian-Triassic palynoflora. Jour. Asian Earth Sci., v.163, pp.1–21.
- Kavali, P. S., Roy, A., di Pasquo M., Gurumurthy G. P, Sharma G., Kumar A. (2021) New age of the Talchir Formation in the Wardha Basin, Central India, based on guide palynomorphs present in radiometrically- dated

- palynozonations in South America, Africa and Australia. *Ameghiniana*, v.58(4), pp.318–344.
- Knoll, A.H. (1985) Exceptional Preservation of Photosynthetic Organisms in Silicified Carbonates and Silicified Peats. *Philos. Trans. Royal Soc. London. Series B. Biological Sciences*, v.311, pp. 111–122.
- Krigstrom, A. (1962) Geomorphological studies of sandur plains and their braided rivers in Iceland. *Geografiska Annaler*, v.44, pp.328–346.
- Lele, K.M. (1979) Studies in the Talchir flora of India-12. Basal Talchir palynofossils from the Penganga Valley and their biostratigraphic value. *Proceedings of the Symposium on evolutionary Botany and Biostratigraphy*, A.K. Ghosh Commemoration Volume, pp.267–283. New Delhi.
- Limarino, C.O., Césari, S.N., Spalletti, L.A., Taboada, A.C., Isbell, J.L., Geuna, S., Gulbranson, E.L. (2014) A paleoclimatic review of southern South America during the late Paleozoic: a record from icehouse to extreme greenhouse conditions. *Gondwana Res.*, v.25,(4), pp.1396–1421.
- MacRae, C.S. (1988) Palynostratigraphical correlation between the Lower Karoo sequence of the Waterburg and Pafuri coal basins and the Hammanskraal plant macrofossil locality, RSA. *Mem. Geol. Surv. South Africa*, v.75, pp.1–217.
- Martínez, M.A., Prámparo, M.B., Quattrocchio, M.E., Zavala, C.A. (2008) Depositional environments and hydrocarbon potential of the Middle Jurassic Los Molles Formation, Neuquén Basin, Argentina: palynofacies and organic geochemical data. *Revista Geológica de Chile*, v.35(2), pp.279–305.
- Mendonça-Filho, J.G., Menezes, T.R., Mendonça, J.O., Oliveira, A.D., Carvalho, M.A., Sant’Anna, A.J., Souza, J.T. (2010) Palinofácies. *In: Souza, C.I. (Ed.), Paleontologia, Interciência*, v.2, pp.379–413. Rio de Janeiro
- Modie, B.N., Le Herissé, A. (2009) Late Paleozoic palynomorph assemblages from the Karoo Supergroup and their potential for biostratigraphic correlation, Kalahari Karoo Basin, Botswana. *Bull. Geosci.*, v.84, pp.337–358.
- Montañez, I.P., Poulsen, C.J. (2013) The Late Paleozoic Ice Age: an evolving paradigm. *Annual Rev. Earth Planet. Sci.*, v.41, pp.629–656.
- Mukhopadhyay, G., Bhattacharya, H.N. (1994) Facies analysis of Talchir Sediments (Permo-Carboniferous), Dudhi Nala, Bihar, India — A glaciomarine model. *Ninth International Gondwana Symposium*, pp.737–753.
- Mukhopadhyay, G., Mukhopadhyay, S.K., Roychowdhury, M., Parui, P.K. (2010). Stratigraphic correlation between different Gondwana basins of India. *Jour. Geol. Soc. India*, v.76, pp.251–266.
- Murthy, S., Kavali, P.S., di Pasquo, M., Chakraborti, B. (2020) Late Pennsylvanian and Early Cisuralian palynofloras from the Rajmahal Basin, eastern India, and their chronological significance. *Historical Biology*, v.32(2), pp.143–159.
- Ogg, J.G., Ogg, G.M., Gradstein, F.M. (2016) *A Concise Geologic Time Scale*. Elsevier, Amsterdam. p.243.
- Pant, D.D. (1996) The biogeography of the late Paleozoic floras of India. *Rev. Palaeobot. Palynol.*, v.90, pp.79–98.
- Parrish, J.T. (1990) Gondwanan paleogeography and paleoclimatology. *In: Taylor T.N., Taylor, E.L. (Eds.), Antarctic Paleobiology*, pp.15–26. New York, Springer-Verlag.
- Peppers, R.A. (1997) Palynology of the Lost Branch Formation of Kansas — new insights on the major floral transition at the Middle–Upper Pennsylvanian boundary. *Rev. Palaeobot. Palynol.*, v.98, pp.223–246.
- Phillips, T.L., Peppers, R.A. (1984) Changing patterns of Pennsylvanian coal-swamp vegetation and implications of climate control on coal occurrence. *Internat. Jour. Coal Geol.*, v.3, pp.205–55.
- Playford, G., Dino, R. (2000a) Palynostratigraphy of upper Palaeozoic strata (Tapajós Group), Amazonas Basin, Brazil: part one. *Palaeontographica*, v.255, pp.1–46.
- Playford, G., Dino R. (2000b) Palynostratigraphy of upper Palaeozoic strata (Tapajós Group), Amazonas Basin, Brazil: part two. *Palaeontographica*, v.255, pp.87–145.
- Roy, A.B., Purohit, R. (2018) Geology of the Gondwana Supergroup. *In: Roy, A.B and Purohit, R. (Eds.), Indian shield: Precambrian evolution and Phanerozoic reconstitution*, pp. 273–285. Elsevier Academic press. Amsterdam.
- Saltzman, M. R. (2003) Late Paleozoic ice age: oceanic gateway or  $p\text{CO}_2$ . *Geology*, pp.31, pp.151–154.
- Scotese, C.R., Song, H., Mills, B.J.W., Van der Meer, D.G. (2021) Phanerozoic paleotemperatures: The Earth’s changing climate during the last 540 million years. *Earth Sci. Rev.*, 103503. doi:10.1016/j.earscirev.2021.103503.
- Shi, G.R., Waterhouse J.B. (2010) Late Palaeozoic global changes affecting high-latitude environments and biotas: An introduction. *Palaeogeog. Palaeoclimat. Palaeoecol.*, v.298, pp.1–16.
- Šimůnek, Z. (2008) The Asturian and Cantabrian floral assemblages with *Cordaites* from the Plzeň Basin Czech Republic. *Studia Geologica Polonica*, v.129, pp.51–80.
- Smith, N.D. (1985) Proglacial fluvial environment. *In: Ashley, G.M., Shaw, J., Smith, N.D. (Eds.), Glacial Sedimentary Environments*, pp. 85–134. Society of Paleontologists and Mineralogists, Tulsa, Oklahoma.
- Souza, P.A., Boardman, D.R., Premaor, E., Félix, C.F., Oliveira, E.J., Bender, R.R. (2021) The *Vittatina costabilis* Zone revisited: new characterization and implications on the Pennsylvanian- Permian icehouse-to-greenhouse turnover in the Paraná Basin, Western Gondwana. *Jour. South Amer. Earth Sci.*, v.106, 102968. doi:10.1016/j.jsames.2020.102968
- Stephenson, M.H. (2008) A review of palynostratigraphy of Gondwana Late Carboniferous to Early Permian glaciogene succession. *Geol. Soc. Amer. Spec. Papers*, v.441, pp.317–330.
- Stephenson, M.H., Angiolini, L., Leng, M.J. (2007) The Early Permian fossil record of Gondwana and its relationship to deglaciation: a review. *In: Williams, M., Heywood, A.M., Gregory, F.J., Schmidt, D.N. (Eds.), Deep-time Perspective on Climate Change: Marrying the Signal from Computer Models and Biological Proxies. The Micropalaeontol. Soc. Spec. Publ.* Geol. Soc. London, pp.169–189.
- Stephenson, M.H, Jan, I.U., Kader Al-Mashaikie, S.Z.A. (2013) Palynology and correlation of Carboniferous–Permian glaciogene rocks in Oman, Yemen and Pakistan. *Gondwana Res.*, v.24, pp.203–211.
- Stephenson, M.H., Leng, M.J., Vane, C.H., Osterloff, P.L., Arrowsmith, C. (2005) Investigating the record of Permian climate change from argillaceous sediments, Oman. *Jour. Geol. Soc. London*, v.162, pp.1–11.
- Tiwari, R.S. (1994) Palynoevent stratigraphy in Gondwana sequence of India, pp. 3-19. *Ninth International Gondwana Symposium Hyderabad, India.*
- Tiwari, R.S., Tripathi, A. (1988) Palynological zones and their climatic inference in the coal bearing Gondwana of Peninsular India. *Palaeobotanist*, v.36, pp.87–101.
- Tiwari, R.S., Tripathi, A. (1992) Marker assemblage zones of spore and pollen species through Gondwana Palaeozoic–Mesozoic sequence in India. *Palaeobotanist*, v.40, pp.194–236.
- Tyson, R.V. (1995) *Sedimentary Organic Matter. Organic facies and palynofacies*. Chapman and Hall, London, 615p.
- Valdez, V.B., Milana, J.P., di Pasquo, M., Paim, P.S.G., Philipp, R.P., Aquino, C.D., Cagliari, J., Junior, F.C., Kellner, B. (2020) Timing of the Late Paleozoic glaciation in western Gondwana: New ages and correlations from Paganzo and Paraná Basins. *Palaeogeog. Palaeoclimat. Palaeoecol.*, v.544, 109624.
- Veevers, J.J., Tewari, R.C. (1995) Gondwana Master Basin of Peninsular India between Tethys and the Interior of the Gondwanaland Province of Pangea. *Geol. Soc. Amer. Mem.*, v.187, pp.1–72.
- Venkatachala, B.S., Tiwari, R.S., Vijaya. (1995) Diversification of spore-pollen character states in the Indian Permian. *Rev. Palaeobot. Palynol.*, v.85, pp.319–340.
- Vijaya (1994) Advent of Gondwanan deposition on Indian Peninsula: a palynological reflection and relationship. *Ninth International Gondwana Symposium, Hyderabad, India*, pp.283–298.
- Vijaya, Tripathi, A., Ram Awatar. (2001) Vertical distribution of spore and pollen index species in the Permian sequence on Peninsular India. *In: Weiss, R.E. (Ed.), Contributions to geology and paleontology of Gondwana – in honour of Helmut Hopfner* (pp. 475–495) Geological Institute, University of Cologne.
- Walter, H. (1985) *Vegetation of the Earth and Ecological Systems of the Geobiosphere*, 3rd edition. Springer-Verlag, New York.
- Zhou, Y.X. (1994) Earliest pollen-dominated microfloras from the early Late Carboniferous of the Tian Shan Mountains, NW China: their significance for the origin of conifers and palaeophytogeography. *Rev. Palaeobot. Palynol.*, v.81, pp.193–211.
- Ziegler, A.M. (1990) Phytogeographic patterns and continental configurations during the Permian Period. *In: McKerrow, W.S., Scotese, C.R. (Eds.), Paleozoic Paleogeography and Biogeography. Geol. Soc. London Mem.*, v.12, pp.363–379.